Eur. J. Mineral.
2011, **23**, 35–43
Published online December 2010

Elasticity of tephroite (α-Mn_2SiO_4) and a comparison of the elastic properties of silicate olivines

CHUNG-CHERNG LIN[1,*] and CHIEN-CHIH CHEN[2]

[1] Institute of Earth Sciences, Academia Sinica, Taipei, Taiwan 115, R.O.C.
*Corresponding author, e-mail: cclin@earth.sinica.edu.tw
[2] Department of Earth Sciences and Institute of Geophysics, National Central University, Chungli, Taiwan 320, R.O.C.

Abstract: The elastic constants of pure tephroite (α-Mn_2SiO_4) have been determined by Brillouin spectroscopy. From measurements, the average aggregate bulk and shear moduli at ambient conditions are 129.8 $\pm$ 0.5 and 53.1 $\pm$ 0.4 GPa, respectively, which also confirm the reality of the unexpected high elastic moduli in tephroite. An analysis based on the present data and those in literature has revealed the relative orders: fayalite $>$ tephroite $\geq$ forsterite for bulk modulus and forsterite $>>$ tephroite $>$ fayalite for shear modulus. It also indicates that the propagation velocity of a sound wave inside forsterite will be considerably changed by dissolving a small amount of Mn^{2+} and/or Fe^{2+} (for shear wave) and Ni^{2+} cations (for compressional wave). The causes for the significant difference between forsterite and the 3d silicate olivines and the unexpected elastic behavior in tephroite have been explored by considering the nature of both electron orbitals and MO_6 octahedra.

Key-words: tephroite, silicate olivines, elastic moduli, effects of cations.

1. Introduction

Iron-bearing forsterite has been considered to be the dominant mineral phase in the Earth's upper mantle. It is known that other silicate olivines (*e.g.*, tephroite, fayalite, γ-Ca_2SiO_4, and Ni-olivine) were also found in nature, and any two of the silicate olivines can form extensive solid solutions (Brown, 1982). Reasonably, the elastic properties of forsterite will be modified together with a change in sound velocity inside the crystal if other M^{2+} cations dissolve in forsterite. Hence, an understanding of the elastic properties of silicate olivines will be helpful to the interpretation of seismological data, in particular the variation in the depth range of transition zone.

Under the given temperature and pressure, Birch (1961) reported that the principal factors determining the velocity (Vp) of a compressional wave in a mineral or rock are the specific mass (*i.e.*, density) and the mean atomic mass ($\overline{M}$) of the concerned material. A linear law correlating Vp with density was suggested for the minerals and rocks having the same $\overline{M}$ (Birch, 1961). In addition, the effects of solutes (impurities) on the elastic properties of a crystal have been attributed to the size of cation (*i.e.*, valence and coordination of cation) (*e.g.*, Anderson, 1969; Prewitt, 1982). These concepts imply that the member having greater molar volume will display lower bulk modulus and hence slower Vp among a group of isostructural compounds. This rule of thumb is valid in several groups, *e.g.*, rock salt-structure 3d (the 3rd transition elements) oxides, alkaline earth oxides (Ohnishi & Mizutani, 1978; Bass, 1995; Knittle, 1995), and calcite-type 3d carbonates (Zhang & Reeder, 1999). Among silicate olivines, most of the measurements for elastic properties have been focused on forsterite, fayalite, and their solid solutions. However, the existed data of bulk modulus for the two olivines are not consistent in their relative order (*e.g.*, the data in Chung, 1971; Yoneda & Morioka, 1992). On the other hand, like the forsterite–fayalite system, continuous solid solution can be formed along the tephroite–forsterite join at one atmosphere pressure. Unusually, the existed data show that tephroite has almost the same bulk modulus and higher shear modulus in comparison with those of fayalite (*e.g.*, the data in Sumino, 1979; Graham *et al.*, 1988; Andrault *et al.*, 1995), though tephroite has larger M^{2+} cation and molar volume. These two cases have confused the people in the mineralogy-related field. Therefore, to clarify the inconsistency observed in the bulk modulus of forsterite and fayalite and check the reliability and actuality of the unexpected high moduli in tephroite, an additional experiment and analysis on the existed data are needed due to its significance to the elastic properties of Fe-and Mn-bearing forsterite and fayalite.

In this study, to clarify the issue about the unexpected elastic behavior of tephroite, the ambient elastic constants of a pure tephroite were measured by Brillouin spectroscopy. This is also the first report for the elastic constants of

0935-1221/11/0023-2077 $ 4.05
DOI: 10.1127/0935-1221/2011/0023-2077

tephroite by Brillouin scattering. To get an overview of the effects of cations on the elastic properties of silicate olivines and explore the possible causes responsible for the unexpected cases mentioned above, if they are true, a systematic comparison based on the present data and those in literature for pure silicate olivines was also carried out.

2. Experimental procedure

To minimize the interference from impurity, high-purity SiO_2 and MnO powder were adopted to synthesize tephroite (α-Mn_2SiO_4) crystals. The oxides were ground thoroughly for mixing and then pressed into tablets. The tablets were put in a Pt container for firing at 1360 °C for 4 h in a suitable CO/CO_2 atmosphere. The as-prepared sample is a pale turquoise sintered polycrystal with 100∼150 μm in grain size. It was confirmed to be tephroite by both X-ray diffraction and Raman spectroscopy. The lattice parameters of this tephroite are: $a = 6.262$ (1), $b = 10.601$ (2), and $c = 4.907$ (1) Å, where values inside the parentheses are the standard deviation. Thus, the X-ray density is 4.1175 g/cm^3, which has been used to calculate the elastic constants and moduli.

The adiabatic elastic constants and moduli of tephroite were measured by Brillouin spectroscopy. The scattered signals were excited by a 514.5-nm Ar^+ laser, and a six-pass tandem Fabry-Pérot interferometer (JRS Scientific Instruments) with a photomultiplier detector was used to collect spectra at ambient conditions (22 °C and 1 atm). For Brillouin scattering experiments, a slice of the sintered polycrystal was ground and polished to a thickness of ∼30 μm. The polished opposite faces of the plates are parallel to each other within ±0.5°. The specimen thus prepared was mounted on a goniometer head of an Eulerian cradle and then adjusted to a symmetric scattering geometry with an external angle of 90° between the incident and scattered beams. With this geometry, the trivial difference in refractive index between the direction of incident ray and that of scattered ray has been usually assumed negligible. Therefore, the refractive index of specimen can be canceled out in the calculation, and the acoustic velocity (V) is calculated by the following formula (Whitfield *et al*., 1976):

$$V = \frac{\lambda \Delta\omega}{\sqrt{2}},$$

where $\Delta\omega$ is the Brillouin shift, and λ is the wavelength of the incident laser. Brillouin spectra were collected from the two sides of the selected crystal to reduce possible errors caused by the non-parallelism of the specimen. The free spectral range (FSR) and finesse are 29.9792 GHz and 120, respectively. To minimize the possible heating on the sample, only 30 mW of laser power was adopted in the measurements. Three grains in the polished polycrystalline specimen at different orientations (based on the interference color of the polished face under crossed nicols) were chosen to measure the elastic constants (C_{ij}s) and moduli of tephroite. Therefore, the data collected in this study were still from single-crystal experiments. An appreciable birefringence was not undergone during measurements. The intensities of Brillouin scattered signals of a crystal are usually orientation-dependent. Hence, a Glan-Taylor prism is used to rotate the polarization of the incident laser beam to 45°, if it is necessary, to obtain better signals at some chi (χ) angles (the angles based on Eulerian cradle). Figure 1 show two typical Brillouin spectra collected in this work. It points out that the quality of some signals at some specific χ angles can be improved by rotating the polarization of the incident laser beam. This can promote the reliability of peak fit. The collection time for a spectrum is 20∼50 min depending on the orientation of phonon involved. Each Brillouin frequency shift was estimated by assuming Gaussian profile for peak fit. The elastic constants and the Voigt-Reuss-Hill aggregate elastic moduli (bulk modulus, K_{VRH}; shear modulus, G_{VRH}) were solved and calculated by a nonlinear inversion procedure adopted in Chen *et al*. (2001) and other places. The acoustic velocities at each χ angle used in the inversion are the averages based on four spectra. The plate plane of the crystal is not parallel to any crystallographic axis. Both C_{ij}s and the normal vector of the crystal plate were simultaneously solved by one inversion until convergence of all physical quantities is attained. Note that the elasticity data determined by Brillouin spectroscopy and various ultrasonic techniques are all adiabatic. Therefore, to use the data collected from single-crystal and polycrystalline samples by using the two types of techniques, both K_{VRH} and G_{VRH} at ambient conditions were replaced by K_{S0} and G_{S0}, respectively, throughout the text.

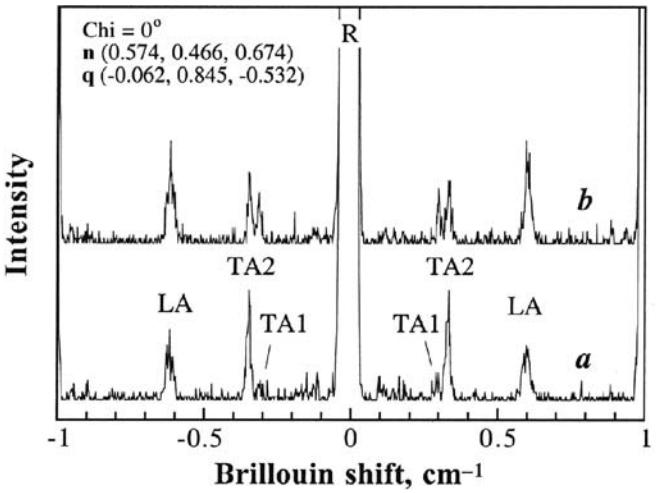

Fig. 1. Brillouin spectra of tephroite at ambient conditions and $\chi = 0°$ without (a) and with (b) the use of Glan-Taylor prism. **n** and **q** are the fitted normal vector of the crystal plate and direction vector of phonon, respectively. LA, longitudinal acoustic mode; TA1 and TA2, transverse acoustic modes; R, Rayleigh scattering.

3. Results

Figure 2 is a set of representative Brillouin data showing the variation of acoustic velocities with the χ angle in a tephroite specimen. According to the data collected from

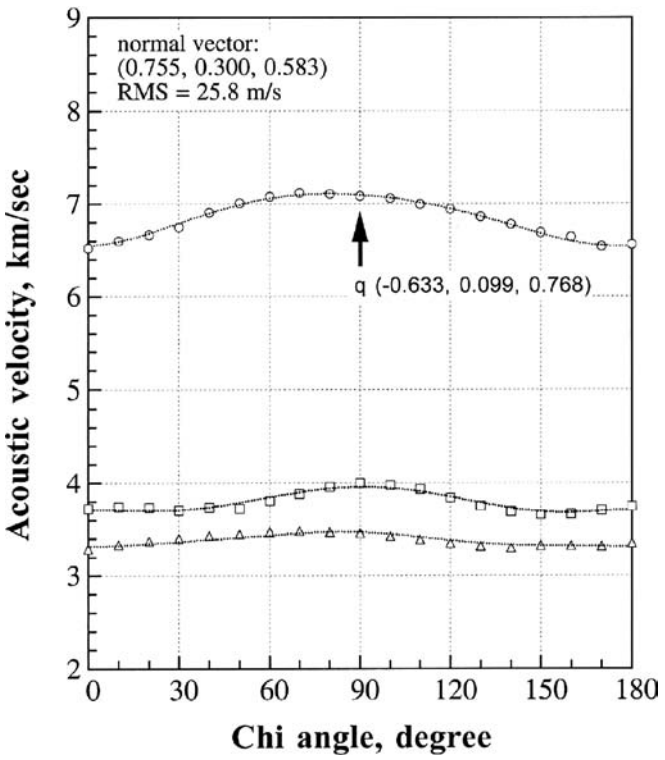

Fig. 2. Longitudinal (circles) and transverse (triangles and squares) acoustic velocities as a function of χ angle for a tephroite specimen at 22 °C. The dotted curves were calculated from the best-fitting C_{ij}s reported in Results. The χ angle is an arbitrary setting mark on the Eulerian cradle, and q denotes the phonon direction at $\chi = 90°$. RMS is the root-mean-square deviation between the calculated and measured velocities.

three crystals, the average of elastic constants of the synthetic tephroite are 246.5 (1.4), 172.9 (0.7), 201 (1.4), 45.1 (0.3), 53.6 (0.7), 56.7 (0.4), 91.9 (0.8), 91.8 (0.8), and 95.3 (0.6) GPa for C_{11}, C_{22}, C_{33}, C_{44}, C_{55}, C_{66}, C_{12}, C_{13}, and C_{23}, respectively. Accordingly, the aggregate bulk (K_{VRH}, K_{S0}), shear moduli (G_{VRH}, G_{S0}) and Poisson's ratio (v) at ambient conditions are 129.8 (0.4), 53.1 (0.3) GPa, and 0.320, respectively. For both C_{ij}s and elastic moduli, the values inside the parentheses are the standard deviation. The K_{S0} and G_{S0} of the present tephroite are less than one percent higher and 2.7 % lower, respectively, than the only data set measured by resonance ultrasonic technique (Sumino, 1979). Therefore, the average elastic moduli of tephroite based on this work and those of Sumino (1979) are 129.3 and 53.9 GPa for K_{S0} and G_{S0}, respectively, and the average of v is 0.317. The C_{ij}s with $i = j$ reported in this study have the same relative order as that reported in Sumino (1979) (*i.e.*, $C_{11} > C_{33} > C_{22} > C_{66} > C_{55} > C_{44}$). However, the orders are different for other C_{ij}s: $C_{23} > C_{12} \approx C_{13}$ in this study and $C_{13} > C_{23} > C_{12}$ in the work of Sumino (1979) (see Table 1). The values of C_{12}, C_{13}, and C_{23} are close to one another. So, the above inconsistency can be attributed to the trade-off during nonlinear inversion. This case is possible if the fitted Brillouin shifts for some orientations deviate from the ideal due to weak or slightly asymmetric signals. In addition, the difference in the relative order of C_{ij}s could be caused by incorrect identification of the acoustic modes in the resonance ultrasonic spectrum (Hong & Vaughan, 1986) or chemical and microstructural inhomogeneities of the specimen coupled with differences in various techniques (Isaak *et al*., 1993). Note that, as mentioned above, both C_{ij}s and the normal of

Table 1. Elastic constants (C_{ij}s) and adiabatic elastic moduli (K_{S0} and G_{S0}) of pure silicate olivines cited in this study (in GPa)[a].

Olivines	C_{11}	C_{22}	C_{33}	C_{44}	C_{55}	C_{66}	C_{12}	C_{13}	C_{23}	K_{S0}	G_{S0}	References
Mg_2SiO_4	330.0	200.3	236.2	67.1	81.6	81.2	66.2	68.0	72.2	128.8	81.7	Isaak et al. (1989a)
	328.4	199.8	235.3	65.2	81.2	80.9	63.9	68.8	73.8	128.6	80.9	Kumazawa & Anderson (1969)
	329.3	199.7	236.7	67.5	81.9	81.3	66.0	68.2	72.1	128.7	81.9	Yoneda & Morioka (1992)
	329.1	200.5	236.3	67.2	81.4	81.1	66.3	68.4	72.8	129.1	81.6	Graham & Barsch (1969),
	—	—	—	—	—	—	—	—	—	128.8	81.6	Zha et al. (1996)5
	—	—	—	—	—	—	—	—	—	128.1	79.7	Chung (1971)6
	—	—	—	—	—	—	—	—	—	128.0	80.0	Li et al. (1996)7
Mn_2SiO_4	258.4	165.6	206.8	45.3	55.6	57.8	87.1	95.2	91.7	128.8	54.6	Sumino (1979)
	246.0	173.5	201.3	45.1	54.3	56.7	91.7	91.6	95.9	129.9	53.3	This work
	246.1	173.5	203.3	45.8	54.1	56.7	90.8	91.7	96.7	130.2	53.5	This work
	245.8	172.1	200.0	44.7	53.0	56.7	91.9	91.7	94.5	129.3	52.8	This work
Fe_2SiO_4	267.0	173.6	239.2	32.4	46.7	57.3	95.2	98.7	97.9	137.9	50.9	Sumino (1979)
	266.0	168.0	232.0	32.3	46.5	57.0	94.0	92.0	92.0	134.0	50.7	Isaak et al. (1993)
	265.9	160.3	222.4	31.6	46.7	57.2	92.4	80.6	88.4	127.5	50.2	Graham et al. (1988)
	267.4	159.8	220.9	31.6	46.7	57.3	92.5	82.0	86.8	127.4	50.3	Graham et al. (1982)
	—	—	—	—	—	—	—	—	—	122.0	53.6	Chung (1971)
	—	—	—	—	—	—	—	—	—	127.7	50.3	Schwab & Graham (1983)
Co_2SiO_4	307.8	194.7	234.2	46.7	63.9	64.8	101.6	105.0	103.2	148.2	62.0	Sumino (1979)
Ni_2SiO_4	340.0	238.0	253.0	71.0	87.0	78.0	109.0	110.0	113.0	164.5	79.5	Bass et al. (1984)
	—	—	—	—	—	—	—	—	—	149.0	85.0	Liebermann (1975)

[a]Except for the reference Zha et al. (1996) for forsterite, the moduli data without a list of C_{ij}s were based on polycrystalline samples.

the crystal plate were solved by one nonlinear inversion at the same time. The errors of C_{ij}s are related to the number of data for inversion. Fewer data for inversion may cause a larger error. Therefore, the inconsistency in the relative order of the C_{ij} between this study and that of Sumino (1979) may be partially ascribed to the fact that only 17 data for each crystal were used in the inversion. Different orders for C_{12}, C_{13}, and C_{23} were also reported for the four sets of ultrasonic data of fayalite (Sumino, 1979; Graham *et al*., 1982, 1988; Isaak *et al*., 1993). On the other hand, $C_{23} > C_{13} > C_{12}$ was reported for the ultrasonic data of pure forsterite (Graham & Barsch, 1969; Kumazawa & Anderson, 1969; Isaak *et al*., 1989a; Yoneda & Morioka, 1992) and the Brillouin data of Ni-olivine (Bass *et al*., 1984). Clearly, this order ($C_{23} > C_{13} > C_{12}$) is still different from that reported in the work of Sumino (1979) for tephroite, fayalite, and Co-olivine. The details of data can be found in Table 1. Nevertheless, compared to the data of Sumino (1979), the present result has indicated that the temperature rise in tephroite due to the absorption of laser is negligible during the collection of spectra.

To understand the effect of cation substitution and to clarify the reality of unexpected elastic moduli observed in tephroite and the inconsistency between the bulk modulus of forsterite and that of fayalite, the data of this study were combined with those of other silicate olivines in literature. Among the methods for getting adiabatic elastic constants and moduli of a solid, various ultrasonic wave-related techniques and Brillouin spectroscopy have been widely adopted by the mineralogy community. It was pointed out that the elasticity data of a sample from both ultrasonic and Brillouin techniques are generally consistent with each other, and a difference as small as <1 % between the two types of methods has been reported (*e.g.*, Vaughan *et al*., 1981; Jackson *et al*., 2006). This indicates that the numerical difference between the two types of data for the same sample is mainly from specimen's condition, the identification of acoustic modes, and inversion procedure as mentioned above rather than the methods themselves. Hence, the elastic moduli of an olivine determined by these methods were combined to obtain the averages. Table 1 lists C_{ij}, K_{S0} and G_{S0} of all pure silicate olivines cited in this study. A comparison of these data is displayed in Fig. 3. The solid circles in Fig. 3 represent the average K_{S0} and G_{S0} based on the data in Table 1, and the error bars indicate the scattering of the data cited. For reference, the average isothermal bulk moduli (K_{T0}) of six silicate olivines were also shown in Fig. 3a (open circles with red error bars). The uncertainty of molar volume for each olivine is about the size of the symbol. All the data cited for Fig. 3 were collected from pure samples (For $\mathbf{K_{S0}}$ and $\mathbf{G_{S0}}$: Graham & Barsch, 1969; Kumazawa & Anderson, 1969; Chung, 1971; Isaak *et al*., 1989a; Yoneda & Morioka, 1992; Li *et al*., 1996; Zha *et al*., 1996 for *forsterite*. Sumino, 1979 and this work for *tephroite*. Chung, 1971; Sumino, 1979; Graham *et al*., 1982; Schwab & Graham, 1983; Graham *et al*., 1988; Isaak *et al*., 1993 for *fayalite*. Sumino, 1979 for *Co-olivine*. Bass *et al*., 1984 for *Ni-olivine*. For $\mathbf{K_{T0}}$: Olinger,1977; Kudoh & Takeuchi, 1985; Will *et al*., 1986; Andrault *et al*., 1995; Downs *et al*., 1996; Zhang, 1998 for *forsterite*. Remy *et al*., 1997 for *Ca-olivine*. Yagi *et al*., 1975; Kudoh & Takeda, 1986; Plymate & Stout, 1990; Knittle, 1995; Andrault *et al*., 1995; Zhang, 1998 for *fayalite*. Zhang, 1998 for both *tephroite* and *Co-olivines*). Therefore, the possible incorrect inference due to the presence of impurities can be avoided. Note that a set of adiabatic moduli for pure polycrystalline Ni-olivine was also reported (Liebermann, 1975; see Table 1). Relative to that from Brillouin scattering (Bass *et al*., 1984), the polycrystalline Ni-olivine showed far smaller bulk modulus and much higher shear modulus. The possible presence of pores inside a polycrystal should deteriorate bulk modulus of the sample, and the presence of grain boundaries will lead to a higher shear modulus in the ultrasonic measurement. Therefore, this data set was not considered further.

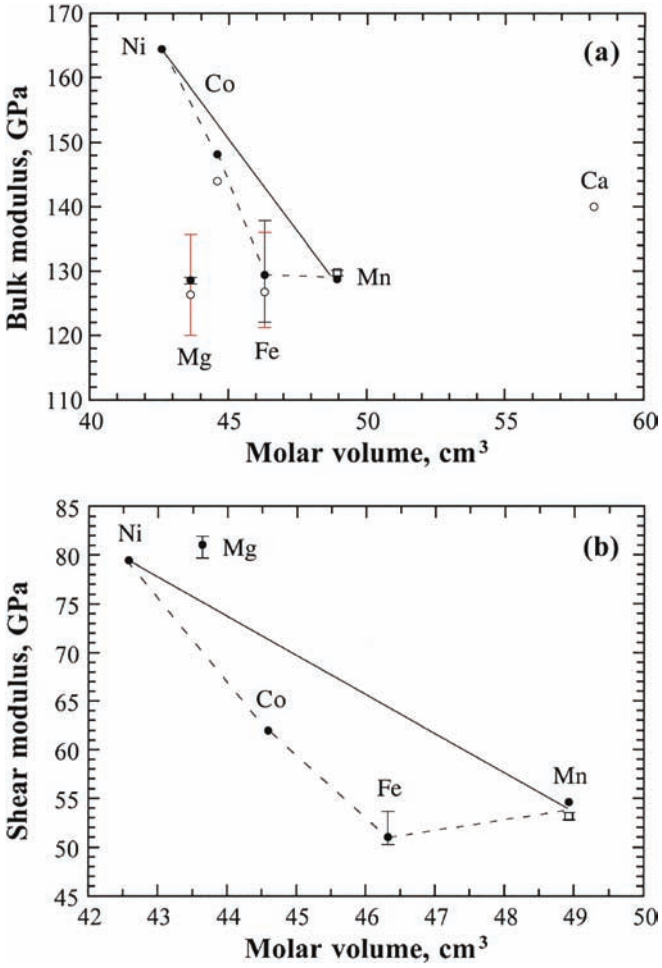

Fig. 3. Adiabatic and isothermal bulk (a) and shear (b) moduli of silicate olivines at ambient conditions. The open circles (with red error bars) denote isothermal bulk modulus (K_{T0}), and solid circles (with black errors) are the aggregate elastic moduli (K_{S0} in (a) and G_{S0} in (b)). The open squares indicate the data of tephroite obtained from this study. The symbols represent the average moduli based on the data cited, and the error bars indicate the ranges of the cited data. The symbols of elements represent the corresponding olivines.

It is noteworthy that the ranges of K_{T0} data for both forsterite and fayalite and that of K_{S0} for fayalite are very

wide. This can be attributed to the following sources: (1) different equations of state, with or without an assumption on the value of pressure derivative of K_{T0}, were taken in data fitting, (2) greater uncertainty in the measurement of lattice parameters was encountered due to small unit-cell change under compression, (3) different methods for X-ray diffraction and the estimation of pressures were adopted, and (4) the quality of specimens, especially fayalite, varied from one study to another. The authors of the current study found that voids usually exist in the synthetic opaque and dark fayalite crystals in addition to the possible presence of twins and microcracks. The imperfections in various fayalite specimens should have resulted in wider data scattering shown in Fig. 3. For forsterite, the range of K_{S0} data (see the black errors) is far narrower than that of K_{T0} (the red error bars). This can be attributed to different methodologies adopted.

4. Discussion

4.1. Elastic moduli of silicate olivines: the effects of cations

4.1.1. Elastic moduli of fayalite and tephroite: a comparison with forsterite

The averages of both K_{S0} (128.6 GPa) and G_{S0} (81.1 GPa) of forsterite in Fig. 3 were based on seven studies (Table 1). The two averages are considered to be highly reliable due to rather narrow scattering of data. All the six K_{S0}s for pure fayalite were measured by ultrasonic wave-related techniques. The significant scattering in the K_{S0} of fayalite can be ascribed to the possible variation in the quality of samples used in these studies. Recently, it was reported that the K_{S0} and G_{S0} of a transparent and near colorless natural fayalite with the composition of $(Fe_{0.94}Mn_{0.06})_2SiO_4$ are 137.57 ± 0.26 and 51.22 ± 0.21 GPa, respectively (Speziale *et al*., 2004). These data are rather close to those of pure fayalite measured by Sumino (1979) ($K_{S0} = 137.9 \pm 1.4$ GPa and $G_{S0} = 50.9 \pm 0.1$ GPa) and were considered to be reliable due to good sample quality. Wang & Bass (1989) also claimed that the elastic moduli of fayalite measured by Brillouin spectroscopy are in good agreement with those of Sumino (1979), though the data were not really published. These results suggest that the K_{S0} of pure fayalite is greater than the average (129.5 GPa) based on the data in literature (*i.e.*, the solid symbol in Fig. 3a), but the average of G_{S0} (51.0 GPa) is close to the true value. The most likely K_{S0} and G_{S0} of fayalite should be *ca*. 138 and 51 GPa, respectively; the former is about the upper limit of K_{S0} in Fig. 3a. Thus, the bulk modulus of fayalite is greater than that of forsterite, but it is the inverse for G_{S0} (Fig. 3b). This conclusion is supported by the existed K_{S0} data for some $(Mg,Fe)_2SiO_4$ solid solutions (Yoneda & Morioka, 1992), the calculated (Liu *et al*., 2010) and the suggested trend for the effect of Fe^{2+} addition on the elastic moduli of forsterite (Sumino, 1979), though a reverse observation was reported by Chung (1971). The observed trend in Chung (1971) is not credible. The possible presence of pores and some unknown factors had caused some problems in the measurement of sintered olivines in Chung (1971).

In Fig. 3, the elastic moduli of tephroite reported in this work (open squares with error bars) and those in Sumino's work (1979) (solid circles) were separately showed. The average K_{S0} (129.3 GPa) of tephroite is slightly higher than that of forsterite (128.6 GPa), while it is the reverse for G_{S0}. This relative order is consistent with that observed in isothermal bulk modulus (Fig. 3a). On the other hand, the average K_{S0} of tephroite shown in Fig. 3a is slightly smaller than that of fayalite. However, according to the above conclusion about the moduli of fayalite, this difference should be greater. As a consequence, the bulk moduli of the three olivines have the relative order: fayalite $>$ tephroite $\geq$ forsterite even if the apparent average K_{T0} of tephroite (127.1 GPa) is slightly higher than that of fayalite (126.8 GPa) (Fig. 3a). Unlike bulk modulus, the average G_{S0} of tephroite (53.9 GPa) based on this study and Sumino's study (1979) is markedly greater than that of fayalite (51.0 GPa, see Fig. 3b) and $(Fe_{0.94}Mn_{0.06})_2SiO_4$ (51.22 GPa). Hence one reaches the conclusion: forsterite $>>$ tephroite $>$ fayalite for shear modulus. Therefore, the present results have confirmed the reality of the unexpected elastic behavior observed in tephroite.

4.1.2. Effects of cations

In Fig. 3, except for tephroite, both K_{S0} and G_{S0} of the 3d olivines decrease with the increase of molar volume, though the dependence appears not linear. The averages of K_{T0}s show a similar trend. However, the elastic moduli of both forsterite and Ca-olivine (γ-Ca_2SiO_4) (*i.e.* the IIA olivines) do not fit to the dependences observed in the 3d olivines. The only K_{T0} data of Ca-olivine (Remy *et al*., 1997) is too high (140 GPa) by taking its far larger molar volume into account. The K_{T0} of pure monticellite ($CaMgSiO_4$) has not been reported. However, two studies on the elasticity of natural Fe-bearing monticellite (molar volume $= 51.44\ cm^3$) showed 113 ± 1, 106 ± 1 and 55.2 ± 0.4 GPa for K_{T0}, K_{S0} and G_{S0}, respectively (Sharp *et al*., 1987; Peercy & Bass, 1990). Hence, by considering the average K_{T0} of pure forsterite (126.4 GPa), the possible K_{S0} of fayalite (138 GPa), and the data of Fe-bearing monticellite, the substitution of Ca for Mg in forsterite should result in a drop of K_{T0}. The abnormally high K_{T0} in Ca-olivine is incorrect, and it can be ascribed to the narrow pressure range for fitting (1–3 GPa) and the possible interference from β phase produced by the $\gamma \rightarrow \beta$ transition at 1.7–2.1 GPa rather than the effect of nonhydrostaticity (Remy *et al*., 1997). Therefore, the bulk moduli of the IIA olivines should decrease with the increase of molar volume, but the dependence is different from that of the 3d olivines.

Based on the analysis in Section 4.1.1, the elastic moduli of fayalite reported by Sumino (1979) and Zhang (1998) (137.9, 50.9, and 136 GPa for K_{S0}, G_{S0}, and K_{T0} respectively) should be the data set being closest to the true values. Thus, it is clear that the dominant factor determining the elastic moduli of a 3d silicate olivine is still molar volume (or unit-cell volume).

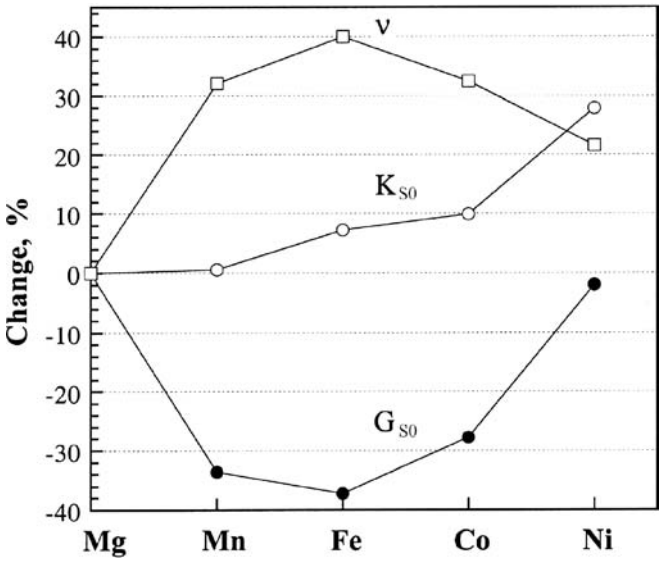

Fig. 4. Variations of elastic moduli of the 3d olivines based on the data of forsterite. Here, change % = 100 × (P_M-P_{Mg}/P_{Mg}), P_M and P_{Mg} represent respectively the elastic moduli of olivine M and forsterite. *v* is Poisson's ratio based on K_{S0} and G_{S0}. The symbols of elements represent the corresponding olivines.

Either bulk or shear modulus of the 3d olivines displays a concave and upward change with molar volume even if the data of Sumino (1979) and Zhang (1998) are taken into account. Using Sumino's data for fayalite, the mean moduli based on this work and that of Sumino (1979) for tephroite (K_{S0} = 129.3 GPa, G_{S0} = 53.9 GPa), and the averages of data in Fig. 3 for other olivines, the effect of cation can be manifested by the variations of elastic moduli as shown in Fig. 4. In Fig. 4, the average of data of forsterite (K_{S0} = 128.58 GPa, G_{S0} = 81.07 GPa, also see Fig. 3) were adopted as reference. Poisson's ratio (*v*, the quotient of lateral contraction divided by longitudinal extension of a substance under tensile stress) reflects the resistance that a substance oppose to volume change with respect to shape change. Compared to forsterite, the greater *v* (or smaller G_{S0}) in all the 3d olivines indicates that the shear deformation in forsterite will become easier by the addition of 3d M^{2+} cations. From forsterite (Mg) to tephroite (Mn), there is a tiny increase in K_{S0} (0.56 %) and significant drop in G_{S0} (33.6 %). This suggests that the influence of an increase in molar volume (10.8 % from forsterite to tephroite) is mainly on shear deformation rather than compression. The considerable increase in molar volume which is accompanied by a slight increase in K_{S0} emphasizes the point that the effect of molar volume is overwhelmed by the change in electronic configuration of M^{2+} cation (from 2p to 3d). This conclusion is also valid as we compare forsterite with other 3d olivines, though forsterite has a molar volume greater than that of Ni-olivine. In Fig. 3b, only one set of data for Ni-olivine is available. Ni- and Mg-olivines would more or less match within the uncertainties if we assume the scattering ranges of data for the two olivines are the same. Nevertheless, in view of the larger molar volume for forsterite, it still indicates that 3d orbital has resulted in a lowering in the G_{S0} of Ni-olivine. In brief, the 3d orbital in cations has caused a drop in the G_{S0} of the 3d olivines in comparison with forsterite. From tephroite (Mn) to fayalite (Fe), an increase in K_{S0} accompanying with an unexpected lowering in G_{S0} was observed. Previously, Peercy & Bass (1990) showed a bulk modulus – cell volume plot for several olivines and Be_2SiO_4. In that plot, the bulk modulus of tephroite also shows a significant positive deviation from the trend defined by fayalite, Co- and Ni-olivines. This result indicates that molar volume is not the sole factor determining the elastic moduli of the 3d silicate olivines. The possible causes for the observed phenomena are explored in the next section.

On the basis of Fig. 3 and 4 and the above discussion, the influence of the substitutional cation on the elastic moduli of forsterite is $Mn^{2+} < Fe^{2+} < Co^{2+} < Ni^{2+}$ for bulk modulus and $Ni^{2+} < Co^{2+} < Mn^{2+} < Fe^{2+}$ for shear modulus. A small amount of Mn^{2+} and/or Fe^{2+} impurities will significantly lower the shear modulus of forsterite, while it just causes a small (for Fe^{2+}) or trivial (for Mn^{2+}) increase in bulk modulus (*e.g.*, 0.5 % increase in K_{S0} and 3.4 % drop in G_{S0} from pure forsterite to $Fo_{93}Fa_7$ (Yoneda & Morioka, 1992)). Whereas, the addition of Ni^{2+} cation will cause an effect opposite to that of Fe^{2+} and Mn^{2+} cations. These mean that the propagation velocity of a seismic wave in the peridotite mantle will be considerably changed by dissolving a small amount of substitutional Mn^{2+} and/or Fe^{2+} (for shear wave) and Ni^{2+} (for compressional wave) cations in olivine.

4.2. Unexpected elastic behavior in tephroite and forsterite – the possible causes

As discussed above, tephroite has a shear modulus greater than that of fayalite, while its bulk modulus shows a markedly positive deviation from the bulk modulus-molar volume dependence defined by the data of fayalite, Co- and Ni-olivines. Forsterite has the greatest shear modulus but the smallest bulk modulus among the olivines concerned (Fig. 3). Previously, Birch (1961) suggested a linear *V*p-density law for the minerals and rocks having almost the same mean atomic mass. The mean atomic mass for forsterite is *ca.* 20.1, while it is 28.85∼29.92 for the 3d olivines. This is a significant difference. Therefore, Birch's approach cannot be applied to explain what observed in Fig. 3. Other factors must be taken into account, except density and mass (or molar volume).

The compressibility of a silicate compound is dominated generally by the contraction of cation polyhedra rather than that of the far stiffer SiO_4 tetrahedra, while shear modulus is significantly related to both deformation of cation polyhedra and the change of M-O-Si angles (M = metal and Si). To understand the causes of the unexpected elastic moduli observed in tephroite and the difference between forsterite and the 3d olivines, a comparison between silicate olivines and rock salt structure oxides (MnO (manganosite), FeO (wüstite), CoO, NiO (bunsenite), MgO (periclase), and CaO (lime)) is helpful because of the same cation coordination for the two groups of compounds. Based on the available experimental data for pure MO oxides, the

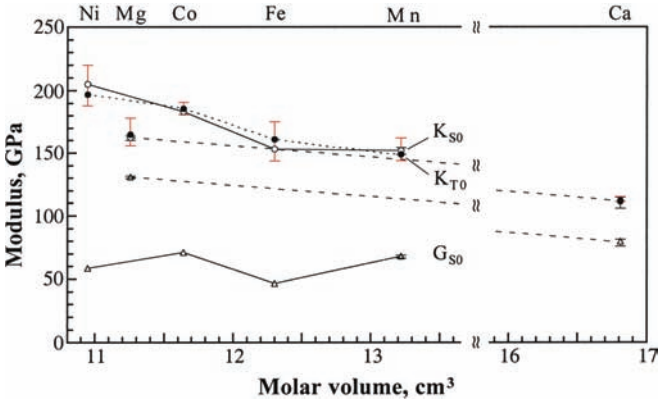

Fig. 5. Adiabatic and isothermal bulk and shear moduli of rock salt-structure MO oxides (M = Mg, Mn, Fe, Co, Ni) at ambient conditions. The solid circles with red error bars denote isothermal bulk modulus (K_{T0}), and open circles (K_{S0}) and triangles (G_{S0}) are the aggregate elastic moduli (with black error bars). The symbols represent the average moduli based on the data cited, and the error bars indicate the ranges of data. The dashed lines link the data of MgO with those of CaO.

modulus-molar volume plots of the rock-salt oxides were depicted in Fig. 5 (**K_{S0}** & **G_{S0}**: Isaak *et al*., 1989b; Bass, 1995; Sinogeikin & Bass, 2000; Li *et al*., 2006; Murakami *et al*., 2009 for *MgO*. Soga, 1968; Son & Bartels, 1972; Bass, 1995; Speziale *et al*., 2006 for *CaO*. Oliver, 1969; Bass, 1995 for *MnO*. Bass, 1995 for *FeO*, *CoO* and *NiO*. **K_{T0}**: Knittle, 1995; Fei, 1999 for *MgO*. Chang & Graham, 1977; Mammone *et al*., 1981; Knittle, 1995 for *CaO*. Ohnishi & Mizutani, 1978; Knittle, 1995; Zhang, 1999 for *MnO*. Ohnishi & Mizutani, 1978; Knittle, 1995; Fei, 1996; Haavik *et al*., 2000; Zhang, 2000 for *FeO*. Ohnishi & Mizutani, 1978; Knittle, 1995 for *CoO*. Ohnishi & Mizutani, 1978; Knittle, 1995; Liu *et al*., 2008 for *NiO*). Note that the average K_{S0}s of MgO, CoO, and FeO in Fig. 5 (the symbols) appear smaller than their K_{T0}s. This case is impossible unless these oxides have negative thermodynamic Grüneisen parameters. The average K_{S0} of MgO should be rather reliable by considering the narrow scattering of data among different studies. The K_{T0} of MgO will be *ca*. 160 GPa if we exclude the data of 178 GPa cited in Knittle (1995) from averaging. Similarly, a smaller K_{T0} (180.9 GPa) was also reported for CoO (see Ohnishi & Mizutani, 1978). On the other hand, the elastic moduli of non-stoichiometric wüstite ($Fe_{1-x}O$) are related to the value of x. Therefore, in Fig. 5, we just cited the data collected from the samples with the smallest deviation from stoichiometry; that is, $Fe_{0.98}O$ and $Fe_{0.99}O$ for K_{T0} and $Fe_{0.95}O$ for K_{S0} and G_{S0}. Compared to K_{S0}, the high average K_{T0} of wüstite should not be true. The K_{T0} of wüstite reported in the two latest measurements is not more than 150 GPa (Fei, 1996; Haavik *et al*., 2000). According to the data collected in Bass' work (1995), a greater deviation in stoichiometry of FeO appears to cause a higher K_{S0} and slightly smaller G_{S0}. However, the K_{T0} of $Fe_{1-x}O$ basically increase with the decrease of x (Hazen & Jeanloz, 1984; Zhang, 2000) or does not vary significantly with composition (Haavik *et al*., 2000). By considering all available data, we suggest the K_{S0} of $Fe_{1-x}O$ slightly drops with the increase of x ($x \leq 0.1$) as that observed in K_{T0}. That is, the ideal FeO have slightly greater K_{S0} and G_{S0} in comparison with those of $Fe_{0.95}O$. Therefore, the use of the data of ideal FeO, if it is available in the future, will not considerably modify the observed trend and the relative position among these oxides shown in Fig. 5.

In Fig. 5, the G_{S0} of CoO may be too high, or the G_{S0} of NiO is too low. An old paper reported a set of even lower K_{S0} and G_{S0} for NiO (Notis *et al*., 1973). Besides, only one set of K_{S0} and G_{S0} data for CoO and FeO was reported till now. To obtain the exact dependence for the G_{S0} of the 3d monoxides, the elastic moduli of these oxides, especially NiO, should be remeasured in the future. Nevertheless, except for MnO, bulk moduli of the 3d oxides decrease basically with the increase of molar volume. The molar volume-elastic moduli dependences of the 3d monoxides are different from those of the alkaline earth oxides (Fig. 5). Both the K_{T0} and K_{S0} of MgO are significantly lower than those of NiO and CoO, whereas, the G_{S0} of MgO is far greater than that of the four 3d oxides. Relative to FeO, a greater G_{S0} in MnO was also observed. Note that the average moduli of MnO are reliable because they were based on four data sets with narrow scattering of data. All these phenomena are basically similar to those observed in silicate olivines (*cf.* Fig. 3 and 5). This suggests that the difference between the elastic properties of forsterite and those of the 3d olivines is mainly resulting from different electron configurations (*i.e.*, the difference in the nature of M–O bonds and cation polyhedra).

The space distribution of *d* orbitals appears more crowded than that of *p* orbitals. From Mg–O to M–O (M=3d cation in olivine), the average bond distance decreases by *ca*. 1 % for M = Ni, and increase by *ca*. 1∼5 % for others (see the data in Smyth & Bish, 1988); however, the number of valence electron in a cation increases 5∼8. Compared to forsterite, the compact 3d orbitals and strong repulsion caused by more valence electrons will make the 3d MO_6 octahedra more incompressible but easy-to-shear and thus greater bulk modulus and smaller shear modulus in the 3d olivines. On the other hand, the shear deformation of a silicate olivine should be correlated chiefly to the distortion of both MO_6 octahedra and the M–O–Si angles rather than the deformation of SiO_4 tetrahedra. It is reasonable that the shorter M-O distances are not in favor of the shearing of MO_6 octahedra in an olivine due to stronger bonding. However, this consideration just suggests that the G_{S0}s of three of the 3d olivines are smaller than that of forsterite (*i.e.*, the easiness for shear deformation of the MO_6 octahedra in silicate olivines is $MnO_6 > FeO_6$, $CoO_6 > MgO_6 > NiO_6$ if M–O distance is the dominant factor). Other factors need be considered to explain the inconsistency between tephroite and fayalite and that between forsterite and Ni-olivine.

Assuming that the radii of oxygen anions in all olivines are the same, the radius ratio of cation to anion (r_M/r_O) will be: $MnO_6 > FeO_6 > CoO_6 > MgO_6 > NiO_6$ for both M1 and M2 sites. It is known that the octahedra in forsterite are not ideal, especially at the smaller M1 sites. By taking the crystal structure of olivine into account, a MO_6 octahedron should be more distortive than MgO_6 if its r_M/r_O ratio is

smaller than that of forsterite. A distorted MO_6 will be sheared easily. Compared to forsterite, this factor together with stronger electron repulsion within Ni^{2+} cation may contribute to the unexpected lowering in G_{S0} of Ni-olivine. For a 3d compound, the pairing energy of 3d electrons in M^{2+} cations inevitably causes higher internal energy and thus lower elastic moduli. However, the strengthening due to a decrease of molar volume and the presence of crystal field stabilization energy (CFSE) can significantly cancel out the effect of pairing energy. These two competitive factors should contribute to the elastic moduli of the 3d olivines. The molar volume and cationic radius of a 3d olivine are interrelated and also reflect the effect of CFSE, if any. The molar volumes of the 3d silicate olivines display almost a linear dependence on the radius (high spin) of M^{2+} cation (not shown). Similarly, linear molar volume-moduli (K_{S0} and G_{S0}) relationships can be found for fayalite and Co- and Ni- olivines if the data of Sumino (1979) for fayalite is adopted. However, both K_{S0} and G_{S0} of tephroite show a positive deviation from the linear dependences constructed by the data of other three olivines. Therefore, relative to fayalite, the unexpectedly higher elastic moduli in tephroite has to be attributed to the absence of paring energy in Mn^{2+}, though the strengthening by CFSE is not involved.

In summary, in addition to molar volume, the pairing energy of 3d electrons and probably CFSE should have contributed to the elastic moduli of the 3d olivines. Both M-O distance and octahedral distortion can be the additional factors influencing the shear modulus of an olivine. The difference in the nature of 3d and 2p orbitals should be the chemical factor claimed by Weidner *et al*. (1982) and Bass *et al*. (1984) for the reverse of the relative order between $(C_{12} + C_{13} + C_{23})$ and $(C_{44} + C_{55} + C_{66})$ in forsterite and the 3d olivines. This study posits that the above interpretation is also valid for the molar volume-modulus dependencies observed in the rock-salt oxides (see Fig. 5).

Acknowledgments: This work was supported by the National Science Council, Taiwan, R. O. C. under contacts NSC 94-2116-M-001-012. The authors thank Dr. H.J. Reichmann and an anonymous referee for valuable comments on the manuscript.

References

Anderson, D.L. (1969): Bulk modulus-density systematics. *J. Geophys. Res.*, **74**, 3857–3864.

Andrault, D., Bouhifd, M.A., Itié, J.P., Rochet, P. (1995): Compression and amorphization of $(Mg,Fe)_2SiO_4$ olivines: an X-ray diffraction study up to 70 GPa. *Phys. Chem. Minerals*, **22**, 99–107.

Bass, J.D. (1995): Elasticity of minerals, glasses, and melts. *in* ''Mineral Physics and Crystallography – A Handbook of Physical Constants'', T.J. Ahrens, ed. AGU, Washington DC, 45–63.

Bass, J.D., Weidner, D.J., Hamaya, N., Ozima, M., Akimoto, S. (1984): Elasticity of the olivine and spinel polymorphs of Ni_2SiO_4. *Phys. Chem. Minerals*, **10**, 261–272.

Birch, F. (1961): The velocity of compressional waves in rocks to 10 kbars, part 2. *J. Geophys. Res.*, **66**, 2199–2224.

Brown, G.E. Jr. (1982): Olivines and silicate spinels. *in* ''Orthosilicates'', P.H. Ribbe, ed. Mineralogical Society of America, Washington DC, chap. 11, 275–381.

Chang, Z.P. & Graham, E.K. (1977): Elastic properties of oxides in the NaCl-structure. *J. Phys. Chem. Solids*, **38**, 1355–1362.

Chen, C.-C., Lin, C.C., Liu, L.-G., Sinogeikin, S.V., Bass, J.D. (2001): Elasticity of single-crystal calcite and rhodochrosite by Brillouin spectroscopy. *Am. Mineral.*, **86**, 1525–1529.

Chung, D.H. (1971): Elasticity and Equations of state of olivines in the Mg_2SiO_4-Fe_2SiO_4 system. *Geophys. J. Roy. Astron. Soc.*, **25**, 511–538.

Downs, R.T., Zha, C.S., Duffy, T.S., Finger, L.W. (1996): The equation of state of forsterite to 17.2 GPa and effects of pressure media. *Am. Mineral.*, **81**, 51–55.

Fei, Y. (1996): Crystal chemistry of FeO at high pressure and temperature. *in* ''Mineral Spectroscopy – A Tribute to Roger G. Burns'', M.D. Dyar, C. McCammon, M.W. Shaefer, eds. The Geochemical Society, Houston, 243–254.

— (1999): Effects of temperature and composition on the bulk modulus of (Mg,Fe)O. *Am. Mineral.*, **84**, 272–276.

Graham, E.K. & Barsch, G.R. (1969): Elastic constants of single-crystal forsterite as a function of temperature and pressure. *J. Geophys. Res.*, **74**, 5949–5960.

Graham, E.K., Sopkin, S.M., Resley, W.E. (1982): Elastic properties of fayalite, Fe_2SiO_4, and the olivine solid solution series. *EOS Trans. AGU*, **63** (45), 1090.

Graham, E.K., Schwab, J.A., Sopkin, S.M., Takei, H. (1988): The pressure and temperature dependence of the elastic properties of single-crystal fayalite Fe_2SiO_4. *Phys. Chem. Minerals*, **16**, 186–198.

Haavik, C., Stølen, S., Hanfland, M., Catlow, R.A. (2000): Effect of defect clustering on the high-pressure behaviour of wüstite: High-pressure X-ray diffraction and lattice energy simulations. *Phys. Chem. Chem. Phys.*, **2**, 5333–5340.

Hazen, R.M. & Jeanloz, R. (1984): Wüstite ($Fe_{1-x}O$): a review of its defect structure and physical properties. *Rev. Geophys. Space Phys.*, **22**, 37–46.

Hong, M. & Vaughan, M.T. (1986): Elasticity of fayalite: a comparison of ultrasonic and paralleipiped resonance data. *EOS Trans. AGU*, **67** (16), 375.

Isaak, D.G., Anderson, O.L., Goto, T. (1989a): Elasticity of single-crystal forsterite measured to 1700 K. *J. Geophys. Res.*, **94B**, 5895–5906.

—, —, — (1989b): Measured elastic moduli of single-crystal MgO up to 1800 K. *Phys. Chem. Minerals*, **16**, 704–713.

Isaak, D.G., Graham, E.K., Bass, J.D., Wang, H. (1993): The elastic properties of single-crystal fayalite as determined by dynamical measurement techniques. *Pure Appl. Geophys.*, **141**, 393–414.

Jackson, J.M., Sinogeikin, S.V., Jacobsen, S.D., Reichmann, H.J., Mackwell, S.J., Bass, J.D. (2006): Single-crystal elasticity and sound velocities of $(Mg_{0.94}Fe_{0.06})O$ ferropericlase to 20 GPa. *J. Geophys. Res.*, **111**, B09203, doi:10.1029/2005JB004052

Knittle, E. (1995): Static compression measurements of equations of state. *in* ''Mineral Physics and Crystallography – A Handbook of Physical Constants'', T.J. Ahrens, ed. AGU, Washington DC, 98–142.

Kudoh, Y. & Takeda, H. (1986): Single crystal X-ray diffraction study on the bond compression of fayalite, Fe_2SiO_4 and rutile, TiO_2 under high pressure. *Physica*, **139/140B**, 333–336.

Kudoh, Y. & Takeuchi, Y. (1985): The crystal structure of forsterite Mg_2SiO_4 under pressure up to 149 kbar. *Z. Kristallogr.*, **171**, 291–302.

Kumazawa, M. & Anderson, O.L. (1969): Elastic moduli, pressure derivatives, and temperature derivatives of single-crystal olivine and single-crystal forsterite. *J. Geophys. Res.*, **74**, 5961–5972.

Li, B., Gwanmesia, G.D., Liebermann, R.C. (1996): Sound velocities of olivine and beta polymorphs of Mg_2SiO_4 at Earth's transition zone pressures. *Geophys. Res. Lett.*, **23**, 2259–2262.

Li, B., Woody, K., Kung, J. (2006): Elasticity of MgO to 11 Gpa with an independent absolute pressure scale: Implications for pressure calibration. *J. Geophys. Res.*, **111**, B11206, doi: 1029/2005JB004251.

Liebermann, R.C. (1975): Elasticity of olivine (α), beta (β), and spinel (γ) polymorphs of germinates and silicates. *Geophys. J. Roy. Astron. Soc.*, **42**, 899–929.

Liu, L., Li, X.D., Liu, J., Jiang, S., Li, Y.C.., Shen, G.Y., Mao, H.K. (2008): High pressure structural and elastic properties of NiO up to 67 GPa. *J. Appl. Phys.*, **104**, 113521.

Liu, L., Du, J., Liu, W., Zhao, J., Liu, H. (2010): Elastic behavior of $(Mg_xFe_{1-x})_2SiO_4$ olivine at high pressure from first-principles simulations. *J. Phys. Chem. Solids*, **71**, 1094–1097.

Mammone, J.F., Mao, H.K., Bell, P.M. (1981): Equation of state of CaO under static pressure conditions. *Geophys. Res. Lett.*, **8**, 140–142.

Murakami, M., Ohishi, Y., Hirao, N., Hirose, K. (2009): Elasticity of MgO to 130 GPa: Implications for lower mantle mineralogy. *Earth Planet. Sci. Lett.*, **277**, 123–129.

Notis, M.R., Spriggs, R.M., Hahn, W.C. Jr. (1973): Elastic, Magnetic, and electric properties of pure and lithium-doped nickel oxide. *J. Appl. Phys.*, **44**, 4165–4171.

Ohnishi, S. & Mizutani, H. (1978): Crystal field effect on bulk moduli of transition metal oxides. *J. Geophys. Res.*, **83B**, 1852–1856.

Olinger, B. (1977): Compression studies of forsterite (Mg_2SiO_4) and enstatite ($MgSiO_3$). *in* ''High Pressure Research: Applications in Geophysics'', M.H. Manghnani & S. Akimoto, eds. Academic Press, New York, 325–334.

Oliver, D.W. (1969): The elastic moduli of MnO. *J. Appl. Phys.*, **40**, 893.

Peercy, M.S. & Bass, J.D. (1990): Elasticity of monticellite. *Phys. Chem. Minerals*, **17**,431–437.

Plymate, T.G. & Stout, J.H. (1990): Pressure-volume-temperature behavior of fayalite based on static compression measurements at 400 °C. *Phys. Chem. Minerals*, **17**, 212–219.

Prewitt, C.T. (1982): Size and compressibility of ions at high pressure. *in* ''High-Pressure Research in Geophysics'', S. Akimoto & M.H. Manghnani, eds. Center for Academic Publication Japan, Tokyo, 433–438.

Remy, C., Andrault, D., Madon, M. (1997): High-temperature, high-pressure X-ray investigation of dicalcium silicate. *J. Am. Ceram. Soc.*, **80**, 851–860.

Schwab, J.A. & Graham, E.K. (1983): Pressure and temperature dependence of the elastic properties of single-crystal fayalite. *EOS Trans. AGU*, **64** (45), 847.

Sharp, Z.D., Hazen, R.M., Finger, L.W. (1987): High-pressure crystal chemistry of monticellite, $CaMgSiO_4$. *Am. Mineral.*, **72**, 748–755.

Sinogeikin, S.V. & Bass, J.D. (2000): Single-crystal; elasticity of pyrope and MgO to 20 GPa by Brillouin scattering in the diamond cell. *Phys. Earth Planet Inter.*, **120**, 43–62.

Smyth, J.R. & Bish, D.L. (1988): Crystal Structures and Cation Sites of the Rock-forming Minerals. Allen & Unwin, Winchester, MA, 332 p.

Soga, N. (1968): Elastic properties of CaO under pressure and temperature. *J. Geophys. Res.*, **73**, 5385–5390.

Son, P.R. & Bartels, R.A. (1972): CaO and SrO single crystal elastic constants and their pressure derivatives. *J. Phys. Chem. Solids*, **33**, 819–828.

Speziale, S., Duffy, T.S., Angel, R.J. (2004): Single-crystal elasticity of fayalite to 12 GPa. *J. Geophys. Res.*, **109**, B12202, doi: 10.1029/2004JB003162.

Speziale, S., Shieh, S.R., Duffy, T.S. (2006): High-pressure elasticity of calcium oxide: a comparison between Brillouin spectroscopy and radial X-ray diffraction. *J. Geophys. Res.*, **111**, B02203, doi:10.1029/2005JB003823.

Sumino, Y. (1979): The elastic constants of Mn_2SiO_4, Fe_2SiO_4, and Co_2SiO_4, and the elastic properties of olivine group minerals at high temperature. *J. Phys. Earth*, **27**, 209–238.

Vaughan, M.T., Manghnani, M.H., Matsui, T. (1981): Single-crystal elastic constants of pure forsterite: a comparison of ultrasonic and Brillouin scattering data. *EOS Trans. AGU*, **62** (17), 392.

Wang, H. & Bass, J.D. (1989): Elastic properties of Fe-bearing pyroxenes and olivines. *EOS Trans. AGU*, **70** (15), 474.

Weidner, D.J., Bass, J.D., Vaughan, M.T. (1982): The effect of crystal structure and composition on elastic properties of silicates. *in* ''High-Pressure Research in Geophysics'', S. Akimoto & M.H. Manghnani, eds. Center for Academic Publication Japan, Tokyo, 125–133.

Whitfield, C.H., Brody, E.M., Bassett, W.A. (1976): Elastic moduli of NaCl by Brillouin scattering at high pressure in a diamond anvil cell. *Rev. Sci. Instrum.*, **47**, 942–947.

Will, G., Hoffbauer, W., Hinze, E., Lauterjung, J. (1986): The compressibility of forsterite up to 300 kbar measured with synchrotron radiation. *Physica*, **139/140B**, 193–197.

Yagi, T., Ida, Y., Sato, Y., Akimoto, S.-I. (1975): Effect of hydrostatic pressure on the lattice parameters of Fe_2SiO_4 olivine up to 70 kbar. *Phys. Earth Planet. Inter.*, **10**, 348–354.

Yoneda, A. & Morioka, M. (1992): Pressure derivatives of elastic constants of single crystal forsterite. *in* ''High-Pressure Research: Application to Earth and Planetary Sciences'', Y. Syono & M.H. Manghnani, eds. Terra Scientific Publishing, Japan, Tokyo, 207–214.

Zha, C.-S., Duffy, T.S., Downs, R.T., Mao, H.-K. (1996): Sound velocity and elasticity of single-crystal forsterite to 16 GPa. *J. Geophys. Res.*, **101B**, 17535–17545.

Zhang, J. (1999): Room-temperature compressibilities of MnO and CdO: Further examination of the role of cation type in bulk modulus systematics. *Phys. Chem. Minerals*, **26**, 644–648.

— (2000): Effect of defects on the elastic properties of wüstite. *Phys. Rev. Lett.*, **84**, 507–510.

Zhang, J. & Reeder, R. (1999): Comparative compressibilities of calcite-structure carbonates: Deviations from empirical relations. *Am. Mineral.*, **84**, 861–870.

Zhang, L. (1998): Single crystal hydrostatic compression of $(Mg,Mn,Fe,Co)_2SiO_4$ olivines. *Phys. Chem. Minerals*, **25**, 308–312.

Received 9 July 2010
Modified version received 30 September 2010
Accepted 25 October 2010